



Hydrogen peroxide-induced oxidative stress and its impact on innate immune responses in lung carcinoma A549 cells

Shishir Upadhyay¹ · Saurabh Vaish¹ · Monisha Dhiman²

Received: 13 November 2017 / Accepted: 11 June 2018 / Published online: 25 June 2018
© Springer Science+Business Media, LLC, part of Springer Nature 2018

Abstract

The immune responses, involved in recognition of cancer-specific antigens, are of particular interest as this may provide major leads towards developing new vaccines and antibody therapies against cancer. An effective treatment for cancer is still a challenge because there are many mechanisms through which the tumor cells can escape the host immune surveillance. Oxidative stress or respiratory burst which is host's mechanism to kill the foreign particles is used as defense mechanism by the tumor cells. The tumor cells uses this oxidative stress to form neo-antigens which in turn makes them undetectable and can escape the host immune surveillance. The human lung carcinoma (A549) cells were treated using 100 μM H_2O_2 to induce oxidative stress, and the extent oxidative modifications were detected at the level of membrane and proteins in form of lipid peroxidation and protein carbonyls respectively. Nitric oxide and iNOS levels were estimated by Griess assay and immunostaining, respectively. The oxidized tumor proteins were visualized on one-dimensional SDS–PAGE. The H_2O_2 -treated (15 min and 24 h post-treatment) A549 cells were co-cultured with THP-1 cells to subsequently visualize the phagocytic activity by Giemsa and CFSE staining to understand the role of neo (oxidized) tumor antigens in eliciting alteration in immune responses. A significant decline in the percent engulfed cells and decrease in the levels of reactive oxygen species was observed. Immunohistostaining for p47^{phox}, which is an important indicator of the oxygen-dependent phagocytosis, showed a decrease in its levels when cells were treated for only 15 min with 100 μM H_2O_2 , whereas at 24-h post-treatment there was no change in the p47^{phox} levels. The study has established oxidative stress as a new pathogenic mechanism of carcinogenesis and will open new avenues for clinical intervention, adjunct therapies for cancer, and its control at the initial stage by targeting these neo-antigens.

Keywords Neo-antigens · Protein oxidation · Respiratory burst · Immune surveillance

Abbreviations

CFSE	5,6-Carboxyfluorescein diester
DAB	3,3'-Diaminobenzidine
DMSO	Dimethyl sulphoxide
DNPH	Dinitrophenylhydrazine
MDA	Malondialdehyde,
MTT	3-(4,5-Dimethylthiazol-2-yl)-2,5-diphenyltetrazolium bromide
NBT	Nitroblue tetrazolium salt

NOX	NADPH oxidases
NO	Nitric oxide
PMA	Phorbol 12-myristate 13-acetate
TBA	Thiobarbituric acid
TBARS	Thiobarbituric acid reactive species

Introduction

Production of reactive oxygen species (ROS) like hydrogen peroxide (H_2O_2), hypochlorite ion (HOCl), hydroxyl radical (OH), superoxide anion ($\text{O}_2^{\cdot-}$), etc., is an inevitable consequence of metabolism (in situ). Besides certain exogenous sources (pollution, cigarette, smoke, radiation, and medication), some endogenous sources are also responsible for the generation of ROS. ROS elevations under normal physiological conditions, due to the default activity of biological scavengers, are required to drive regulatory pathways [1].

✉ Monisha Dhiman
monisha.dhiman@gmail.com; monisha.dhiman@cup.edu.in

¹ Department of Animal Sciences, School of Basic and Applied Sciences, Central University of Punjab, Bathinda, Punjab, India

² Department of Biochemistry and Microbial Sciences, School of Basic and Applied Sciences, Central University of Punjab, Bathinda, Punjab 151 001, India

However, the higher levels of intracellular ROS (beyond a threshold) can lead to apoptosis or necrosis [2]. Chronic and degenerative ailments including, autoimmune disorders, aging, cataract, rheumatoid arthritis, cardiovascular diseases, neurodegenerative disorders, and cancer-associated complications arise due to perturbed ROS equilibrium [3].

ROS is a double-edged sword which can either suppress or promote the cancerous growth [1]. The chemical entities can prolong the cell survival and contribute to malignant transformation [4, 5] in multiple ways, right from the oral cavity [6] to lung [7], breast [8], prostate [9], gut [2], and ovarian tissues [7], and also play a role in hepatitis B/C virus-induced hepatocellular carcinoma [10]. These by-products of oxidative stress induce conformational changes in DNA, proteins, and lipids which if not degraded by the ubiquitin–proteasome system can further result in glycosylation, glycation, phosphorylation, or oxidation which affect the function and stability of biomolecules [11]. ROS can react with cysteine, histidine, lysine, arginine, proline, or threonine residues of proteins to produce carbonyls [12]. Similarly, lipid peroxidation due to ROS production during various pathophysiological conditions generates malondialdehyde (MDA) and 4-hydroxynonenal. These resulting products are known to promote cell proliferation and block apoptotic pathway [13]. Identifying these oxidized products of the macromolecules can, therefore, serve to determine the extent of oxidative stress induced during an abnormal physiological condition.

The immune defense mechanisms and their interaction with the tumor microenvironment are another important aspects where the tumor immune escaping can be considered [14]. The macrophage-mediated innate immune responses are important to detect and kill the tumor. Macrophages constitute a major portion of the infiltrate surrounding the tumor; they interact with modified extracellular matrix (ECM) proteins, and instead of killing, at times can favor the tumor development. Due to high inflammatory molecules such as iNOS, COX2, and proinflammatory cytokines in the tumor microenvironment, the tumor supporting cells such as tumor-associated macrophages (TAM) are formed which stimulate the migration and metastasis of cancer cells by secreting Epidermal Growth Factor [15] and by expressing the receptor for Colony Stimulating Factor 1 [16]. ROS can also account for the phenotypic plasticity of macrophage and can downregulate the immune responses via neo-antigen formation [17, 18]. The altered antigens, generated while apoptosis and/or oxidation of proteins and lipids, can indulge in tumor resistance to radiotherapies and host immune system [19–21]. The chemical changes in amino acid residues induced by ROS can alter the coding sequences as well as tertiary and quaternary organization of a protein. These mutated peptides might create new epitopes, called as neo-antigenic determinants. Neo-antigens display a modified version of the usual antigenic determinant, and that is why, they require a different,

specific antibody for recognition [22]. The neo-antigens are the characteristics of autoimmune pathogenesis as well as cancer, and can be detected by Serological expression cloning (SEREX) and ELISPOT. Somatic mutations and neo-antigen density has recently been shown to cooperate in the progression of non-small cell lung cancer. Further, the patients with higher mutation burden or neo-antigen load were suggested to be correlated with an enhanced clinical response. As a high tumor mutation is associated with increased neo-antigens and tumor-infiltrating lymphocytes, these mutations can act as potential biomarkers for deciding the efficacy of cancer immunotherapy. In this context, there are success reports available for colorectal and other cancers, but a fewer for lung cancer [23–25]. In brief, oxidative stress triggers cellular damage as well as boosts the inflammatory response, both of which can decrease the phagocytic activity of the activated macrophages towards apoptosis of cancer cells [26]. In the present study, we aimed to investigate that whether oxidative environment can aid the escape of cancer cells from phagocytic defenses. Our central hypothesis is that the oxidative stress may alter tumor proteins resulting in the formation of novel epitopes, which if not recognized by the host immune system, due to being neo-antigens, may lead to accumulation of tumor cells resulting in carcinogenesis. The *in vitro* system of the human lung carcinoma cell line (A549) is utilized as a model for inducing oxidative modification using H_2O_2 as an oxidant. The subsequent response towards oxidative stress is realized based on the macromolecular damage, and respiratory burst, and phagocytic activity. Our study will pave the unique role of ROS which by forming neo-antigens on tumor cells if identified may open new avenues for clinical intervention and adjunct therapies for cancer.

Materials and methods

Cell culture

Human lung carcinoma A549 cells were procured from National Center for Cell Sciences (NCCS), Pune, India, and were grown in complete media DMEM supplemented with 10% FBS in 5% CO_2 humidified incubator. Human monocytic leukemia THP-1 cells were generously gifted by Prof. Kanuri Rao, ICGEB, New Delhi, India. Morphologically, THP-1 cells are large, round single cells grown in suspension and differentiated into macrophages on stimulation with PMA. The suspension THP-1 cells were maintained in RPMI 1640 medium with 2 mM L-glutamine, 1.5 g/L $NaHCO_3$, 4.5 g/L glucose, 10 mM HEPES, and 1.0 mM sodium pyruvate and supplemented with 0.05 mM of 2-mercaptoethanol and 10% FBS. THP-1 cells were treated with 10 ng/ml PMA for 48 h to induce terminal differentiation of these cells into macrophages which then show adherence.

Cell treatments and preparation of cell lysates

A549 cells (1×10^6) were seeded and treated with H_2O_2 (100 μ M) for 24 h in serum-starved conditions. For the co-culturing experiments, the A549 cells were treated with 100 μ M H_2O_2 for 15 min to see its effect at initial stages as soon as it enters the cells and for 24 h to see the effect of H_2O_2 after the oxidative stress is induced to bring any change in the macromolecules. After the treatment, the culture supernatant was stored and cell lysate was prepared using lysis buffer 20 mM Tris–HCl (pH 7.2), 250 mM sucrose, 0.6% Nonidet P-40, 2 mM EGTA, 40 mM KCl, 0.5 mM PMSF, 10 mM leupeptin, and 10 mg/ml aprotinin. Amount of protein in the samples was estimated using Bradford's assay and the aliquots of cell lysates were stored at -80°C till further use.

Cytotoxicity assay

A549 cells (1×10^5) plated in 24-well plates were treated with different concentrations of H_2O_2 (0, 20, 50, 100, 150, 200 μ M) in FBS-free media. After 24 h, 20 μ l of MTT solution (5 mg MTT dissolved in 1 ml sterile PBS) was added followed by incubation for 4 h at 37°C . The purple product was solubilized using 200 μ l of 10% SDS in acidified DMSO and absorbance was measured at 570 nm. The absorbance read is directly proportional to number of living cells [27]. The percent cell viability of each group was calculated with respective controls.

Detection of neo-antigens

A549 cell lysates from all the treated and untreated groups (20 μ g of protein) were resolved on 10% SDS–PAGE on a Mini-Protean 3 system (Bio-Rad) using 0.2 mol/L Tris–HCl anode buffer (pH 8.8) and 0.1 mol/L Tris–Tricine cathode buffer containing 0.1% SDS. Gels were stained with 0.05% Coomassie blue G250, and images were acquired using advanced gel documentation system (Bio-Rad).

Detection of protein carbonyls

A549 cell lysates (50 μ g) were derivatized with DNPH (100 mM in 2 M HCl) at 37°C for 90 min. Protein precipitation was done with TCA (28%) followed by washing with ethanol and ethyl-acetate solution (1:1). After final washing, the samples were centrifuged at 6000 rpm for 6 min and the pellet resuspended in 6 M guanidine HCl. The absorbance was read at 360 nm using spectrophotometer (Shimadzu UV-2450). The amount of protein carbonyls were determined by using an extinction coefficient of $21,000\text{ M}^{-1}\text{cm}^{-1}$ and expressed as nanomoles (nmols) of protein carbonyls per mg of protein. For Western blotting, protein sample (35 μ g)

from untreated control and treated group were derivatized with 20 mM DNPH at 37°C for 30 min followed by neutralization with 4M Tris–HCl and 30% Glycerol (pH 6.8 and). The derivatized samples were separated on 10% SDS–PAGE and proteins transferred to nitrocellulose membrane at 4°C . Membranes were blocked for 2 h with 1% BSA washed and incubated overnight at 4°C with rabbit Anti-DNP (1:1000; Santa Cruz) followed by incubation with HRP-conjugated goat anti-rabbit secondary antibody (1:5000; Santa Cruz) for 2 h. Enhanced chemiluminescence (ECL) reagent was used as a chemiluminescent substrate to detect the signal followed by imaging and data analysis using Bio-Rad Chemi-Doc imaging system.

Thiobarbituric acid reactive species (TBARS) estimation

A549 cell lysates (50 μ g) were mixed thoroughly with 15% (w/v) trichloroacetic acid (TCA), 0.375% (w/v) TBA, and 0.25 mol/L HCl. The reaction mixture was heated for 30 min in boiling water bath and the flocculent precipitate was removed by centrifugation at 1000 rpm for 10 min. The absorbance of the supernatant was determined at 530 nm, and the TBARS concentration was calculated using $1.56 \times 10^5\text{ M}^{-1}\text{cm}^{-1}$ as molar absorption coefficient, and results were expressed as nanomoles (nmols) per mg of protein.

Nitric oxide assay

The extracellular NO levels were assayed by using 100 μ l of fresh cell culture supernatants of treated (100 μ M H_2O_2) and untreated controls incubated with equal volume of Griess reagent (1% sulphanilamide, 5% phosphoric acid, and 0.1% N-[1-naphthyl] ethylenediamine dihydrochloride). The optical density was measured at 545 nm. The nitrate content was evaluated from the standard curve of NaNO_3 [28]. The intracellular iNOS/NOS2 localization and expressions were detected by using immunostaining. 2×10^5 A549 cells were seeded on glass coverslips in six-well plate; after 24 h the medium was removed from the wells and cells were washed three times with $1 \times$ PBS. The cells were fixed with 2% paraformaldehyde for 10 min in dark and permeabilized with 0.1% Triton X-100 for 5 min, then cells were blocked with 10% FBS for 1 h at 37°C followed by incubation with Anti-NOS2 (iNOS) primary antibody (1:100, Santa Cruz) for overnight at 4°C in a humidified chamber. The antibody binding was detected with FITC-labeled Anti-IgG Alexa Fluor-647 secondary antibody (1:200, Invitrogen). The nuclei of cells were stained with DAPI for 30 min. The coverslips were then mounted on microscopic glass slides and the immunofluorescence images were obtained using Olympus FV-1200 Laser Scanning Confocal Microscope

(Olympus) at Central Instrumentation Laboratory (CIL), Central University of Punjab, Bathinda.

Phagocytosis assays

Giemsa staining

1×10^5 A549 cells were treated with H_2O_2 for 15 min and 24 h. A total 0.5×10^5 THP-1 cells were allowed to differentiate into macrophages with PMA (10 ng/ml) treatment at $37^\circ C/5\% CO_2$ in a Lab-Tek II chamber slides. THP-1 cells were then co-cultured with A549 cells (2:1 ratio) for overnight. Cells were fixed in absolute methanol (200 μ l) for 5 min, and stained with Giemsa stain (1:20, v/v) for 20 min to visualize the macrophages and tumor cell uptake. Images were visualized under light microscope (CX25 OLYMPUS) at $100\times$ [20]. The percentage of engulfed cells was calculated by number of cells engulfed per total number of cells.

CFSE assay

1×10^5 A549 cells were treated with H_2O_2 for 15 min and 24 h. Cells were trypsinized and stained with CFSE (16 μ M/PBS) at $37^\circ C/5\% CO_2$ for 30 min. The A549 cells were then washed with PBS to remove the unbound dye and CFSE-stained cells were co-cultured overnight with PMA-differentiated THP-1 cells as described above in the Lab-Tek II chamber slides. The fluorescent cells which get phagocytosed by macrophages were visualized under CX25 OLYMPUS microscope. The percentage of engulfed cells was calculated by number of cells engulfed per total number of cells.

Respiratory burst assays

NBT assay

PMA-treated THP-1 cells (1×10^5) were co-cultured with control, untreated, and H_2O_2 (100 μ M)-treated A549 (1×10^5) cells for 15 min and 24 h in a six-well plate. After 24 h, 0.1% NBT (500 μ l) was added and plates were incubated at $37^\circ C/5\% CO_2$ in the dark. After 45 min, the NBT was removed washed and DMSO and 2M KOH was used to dissolve the crystals. Absorbance was measured at 570 and 630 nm [20].

Immunohistochemistry for p47^{phox}

Control and H_2O_2 -treated A549 cells were co-cultured with PMA-differentiated THP-1 in the Lab-Tek II-chambered slides for overnight. After washing with PBS, the cells were fixed with chilled acetone for 5 min and air dried. All the slides were then treated with 0.3% H_2O_2 /PBS for 15 min.

Then the blocking reagent (1% BSA/PBST) was added for 30 min. All slides were then washed twice, added p47^{phox} mouse antibody (1:500, Santa Cruz) for 1 h at room temperature, and washed again with PBST. Followed by incubation for 30 min with anti-mouse-HRP-conjugated secondary antibody (1:1000, Santa Cruz), DAB (5 mg/10 ml) and 10 μ l of 3% H_2O_2 were added for color development and counterstained with Mayer's hematoxylin (Invitrogen) and again washed with water and air dried. Finally, all the slides were mounted in DPX and images were taken in the CX25 OLYMPUS microscope. The percent positive cells were calculated by number of cells showing positive staining per total number of cells seeded [29].

Statistical analyses

All assays were repeated at least thrice. Data were presented as mean \pm SD for control as well as experimental samples. For all statistical comparison, Student's *t* test was used with *p* value < 0.05 considered as statistically significant.

Results

Effect of H_2O_2 on cell viability

The response of H_2O_2 was determined by treating A549 cells with different concentrations of H_2O_2 (0–200 μ M) for 24 h (Fig. 1). The A549 cells when treated with 50 μ M of H_2O_2 showed no significant difference in percent viability as compared to the untreated control cells ($83.1\% \pm 32.1$ and $87.0\% \pm 35.4$ vs. 100, respectively). However, 200 μ M concentration of H_2O_2 showed significant decline in cell viability when compared to untreated control cells ($63.1\% \pm 8.6$ vs. 100, respectively) while 100 and 150 μ M H_2O_2 showed a moderate to minimal toxicity to cells ($78.9\% \pm 19.7$ vs. 100, respectively). In further experiments, 100 μ M H_2O_2 concentration was used as an oxidative stress inducer in A549 lung cancer cells.

H_2O_2 induced neo-antigen formation

Protein modifications which occur in the cells following oxidative stress might be responsible for the neo-antigen formation. In order to detect the neo-antigens, the H_2O_2 -treated and control cell lysates (20 μ g of protein) were resolved on 10% polyacrylamide gel. Figure 2 shows the gel stained with Coomassie brilliant blue (CBB) depicting bands that were observed only in H_2O_2 -treated samples (marked with arrows) while, the corresponding bands were not visible in the control cell lysate suggesting the formation of oxidized neo-antigens or modified proteins. In vitro oxidized BSA was used for positive control.

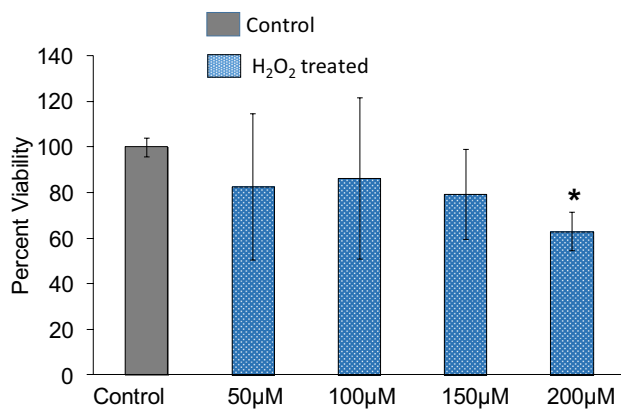


Fig. 1 Effect of H₂O₂ treatment on A549 cells. The A549 cells were treated with various concentrations of H₂O₂ (0–200 µM) and the cell viability was estimated by MTT assay. The data presented as percent viability of A549 cells when treated with increasing concentrations of H₂O₂. The results are expressed percent change \pm standard deviation ($n=3$). Student *t* test was performed to evaluate the significance of the results, the data were considered as statistically significant at $*p \leq 0.05$ when H₂O₂ treated cells were compared with untreated controls

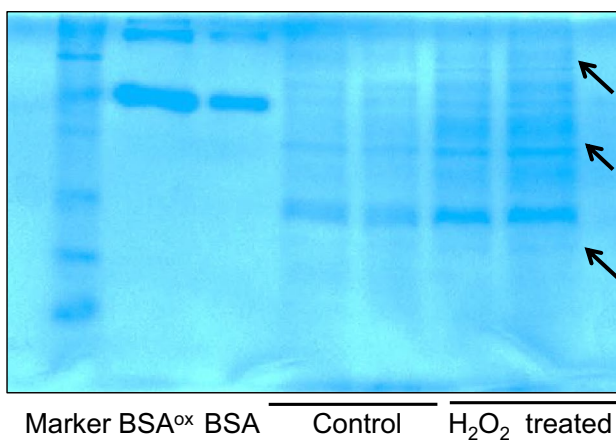


Fig. 2 Neo-antigen detection. The A549 cells treated with 100 µM of H₂O₂. The cell lysates were prepared and resolved on a SDS-PAGE then stained with Coomassie Brilliant Blue. Lane 1: marker (Protein ladder as size standard); Lane 2: BSA^{ox} (Positive control); Lane 3: BSA; Lane 4 and 5: control (without treatment); Lane 6 and 7: H₂O₂-treated samples (100 µM)

H₂O₂ induced protein carbonyls formation

Protein carbonyl content is a measure of oxidative damage in proteins produced due to ROS. Hydrazones formed after reaction of DNPH and carbonyls (by-product of protein oxidation) were estimated by spectrophotometric method. A significantly high protein carbonyl control (20.6 ± 7.4) was observed for H₂O₂-treated cell lysates (24 h) when compared with untreated controls (7.7 ± 1.2) (Fig. 3a) which indicates that the oxidative stress induced protein modification due

to the H₂O₂ treatment. Western blot showed a significant increase in protein carbonyl content in 100 µM H₂O₂-treated cell lysates for 24 h as compared to 100 µM H₂O₂-treated cell lysates for 15 min. Both derivatized oxidant-treated samples showed high content of protein carbonyls as compared to their respective derivatized untreated control for 15 min and 24 h (Fig. 3b-i). Densitometric analysis of Western blot showed twofold increase in carbonyl content in 100 µM H₂O₂-treated cell lysates after 24 h, indicating increased protein oxidation as compared to the untreated control cells (Fig. 3b-ii).

H₂O₂ induced lipid peroxidation

Oxidative stress might lead to oxidation of lipids present in cell membrane resulting in the reaction of malondialdehyde (MDA) with thiobarbituric acid (TBA) resulting in the formation of thiobarbituric acid reactive species (TBARS). Control and H₂O₂ (100 µM)-treated A549 cell lysates were examined for lipid peroxidation, Fig. 3c shows a significant increase of 64.8% in lipid peroxidation level in H₂O₂-treated cell lysates.

H₂O₂ induced NO generation

NOS2 is often associated with NO generation which is further responsible for inflammation and may cause modification of certain other proteins in tumor cells via different mechanisms and thereby forming additional neo-antigens. To see the extracellular and intracellular generation of NO, Griess assay and confocal microscopy were performed. It was observed that 100 µM H₂O₂-treated A549 cells showed higher extracellular NO levels as compared to untreated A549 cell culture supernatants (Fig. 3d-i, d-ii, Table 1). The intracellular expression of NOS2/iNOS in 100 µM H₂O₂-treated A549 cells was elevated as compared to their respective controls (Fig. 3d-ii).

Immune escape by tumor cells

The PMA-differentiated THP1 macrophages were co-cultured with control and 100 µM H₂O₂-treated A549 cells, and the extent of innate immune response in the form of phagocytic activity and/or respiratory burst was determined.

Effect of neo-antigen formation on phagocytosis

Phagocytosis is an innate immune response exhibited by macrophages thereby engulfing the foreign particles. Neo-antigens formed due to oxidative stress may help tumor cells evade the host's immune response.

A549 cells were treated with 100 µM H₂O₂ for 15 min and 24 h followed by co-culturing with the THP-1 cells and were

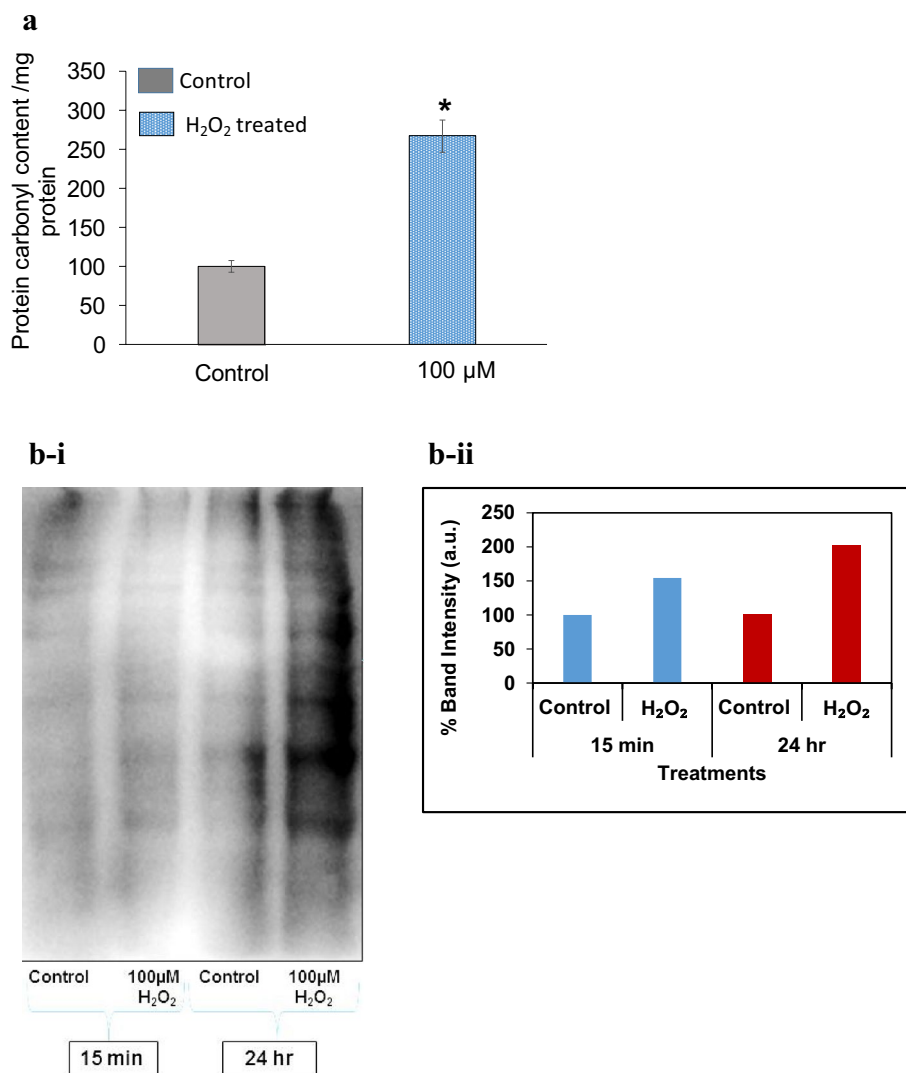


Fig. 3 Detection of oxidative stress and nitrosative stress. **a** Protein Carbonyls. The protein carbonyl content of control and H_2O_2 -treated (100 μ M) A549 cells was assessed with DNPH assay as described in “Materials and methods.” The amount of protein carbonyls was detected in terms of nanomol of protein carbonyls per mg of protein when compared with untreated control A549 cell lysates. The results are expressed as the mean \pm standard deviation ($n=3$). Student t test was performed to evaluate the significance of the results, the data were considered as statistically significant at $*p \leq 0.05$ when H_2O_2 -treated cells were compared with untreated controls. **b-i** Western blot analysis of protein carbonyls in A549 cells: blot showing protein oxidation in A549 cells treated with 100 μ M H_2O_2 , where figure represents the derivatized samples for two time points 15 min and 24 h. **b-ii** Densitometric analysis of Western blot of derivatized protein carbonyls in A549 cells. **c** Thiobarbituric Acid Reactive Species (TBARS) Estimation. The lipid peroxidation content of control and H_2O_2 -treated (100 μ M) A549 cells was assessed with TBARS assay. The amount of lipid peroxidation was estimated in nanomol of per mg of protein when compared with untreated control A549

cell lysates. The results are expressed as the mean \pm standard deviation ($n=3$). Student t test was performed to evaluate the significance of the results, the data were considered as statistically significant at $*p \leq 0.05$ when H_2O_2 -treated cells were compared with untreated controls. **d-i** Detection of extracellular NO levels in A549 cell culture supernatants. Extracellular NO was detected using Griess assay in 100 μ M H_2O_2 -treated A549 cell culture supernatants for 24 h. Student t test was performed. The results are expressed as the mean \pm standard deviation ($n=3$). Student t test was performed to evaluate the significance of the results, the data were considered as statistically significant at $*p \leq 0.05$ when H_2O_2 -treated cells were compared with untreated controls. **d-ii** Detection of H_2O_2 -induced intracellular NOS2/iNOS in A549 cells. The cells were treated with 100 μ M H_2O_2 for 24 h time points and the NOS2 (iNOS) was localized by using immunofluorescence staining. Images were taken at a magnification of 60 \times using Olympus FV-1200 Laser Scanning Confocal Microscope (Olympus) [Control (A–C); 100 μ M H_2O_2 Treated 15 min (D–F)]

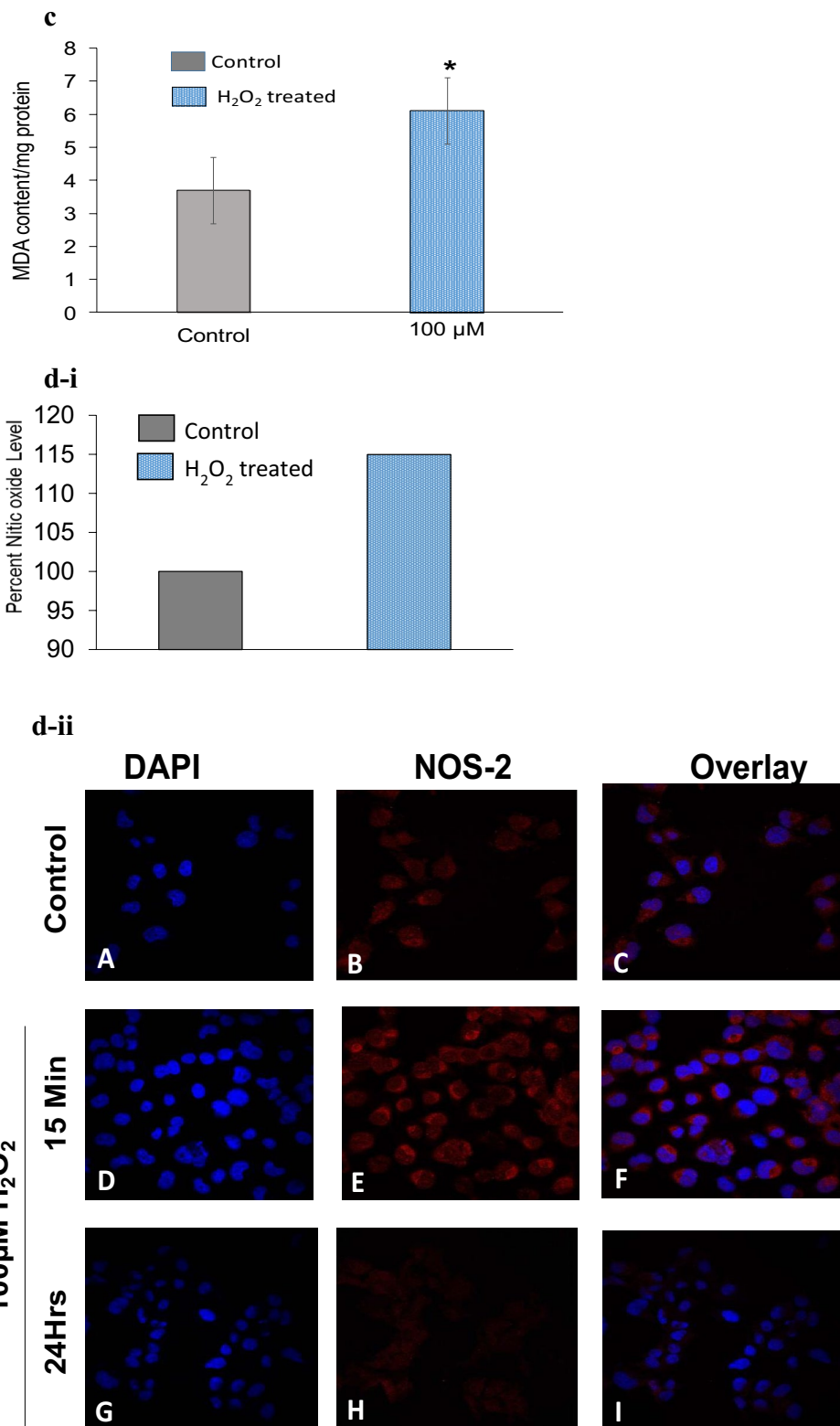


Fig. 3 (continued)

Table 1 Extracellular NO levels in the 100 μM H_2O_2 -treated A549 cell culture supernatants

A549 cell culture supernatants	Percent NO generation
Control	100 \pm 0
100 μM H_2O_2	114.97 \pm 13.72

Table shows the percent NO levels (arbitrary units)

subsequently visualized for the presence of phagocytic activity by Giemsa staining under light microscope (Fig. 4a). Figure 4b depicts a significant 85% decline in percent engulfed cells in 24-h-treated cells, whereas A549 cells when treated for 15 min the proportion of engulfed cells was similar to the untreated control cells (Table 2).

As a second measure, CFSE-stained A549 cells were co-cultured with THP-1 cells to measure the phagocytosed cells using fluorescent microscope (Fig. 4c). The bright green-stained cells correspond to the free A549 cells which are not engulfed by THP-1 cells, whereas the engulfed A549 cells can be seen inside the THP-1 cells. The A549 cells treated for 24 h with H_2O_2 showed 46% decline in number of engulfed cells when compared to the control, whereas the A549 cells when treated for 15 min with H_2O_2 did not show any change as compared to untreated control cells (Table 2; Fig. 4d).

Effect of neo-antigen formation on respiratory burst

Respiratory burst is another defense mechanism of innate immune cells in response to foreign particles during phagocytosis. The phagocytosis-generated ROS is responsible for killing the cancerous cells and foreign particles. Keeping this in view, we measured ROS levels by NBT assay in macrophages and immunostaining for NADPH oxidase subunit p47^{phox}. A significant decrease of 25 and 36% in ROS levels was observed in THP1 cells co-cultured with A549 cells treated when treated with H_2O_2 for 15 min and 24 h, respectively, when compared with the untreated control (Fig. 5; Table 3).

P47^{phox} is the cytosolic unit of NADPH oxidase which is one of the most important enzymes of the oxygen-dependent phagocytosis. Immunohistostaining was performed to detect the p47^{phox} levels. The A549 cells treated with H_2O_2 for different time intervals were co-cultured with THP-1 cells and subsequently immunostained for p47^{phox} (Fig. 6a). The THP-1 cells co-cultured with H_2O_2 -treated A549 cells for 15 min showed a significant decrease of 55% in immunostaining, whereas there was no change when the A549 cells were treated for 24 h. These results suggest that during phagocytosis, the NADPH oxidase enzyme does not get compromised and its function is not impaired in the 24 h H_2O_2 -treated A549 cells (Fig. 6a, b; Table 4).

Discussion

Malignant tumors of the lungs are the most prevalent oncological diseases making lung cancer one of the leading causes of deaths due to cancer [30]. ROS resulting from inflammation and other stresses are among the major factors responsible for the lung cancer incidences [31]. ROS accumulate in the form of oxidative stress and consequently triggers adaptive changes at molecular level. Cellular macromolecules suffer innumerable damages through ROS overproduction, which in turn can stimulate various signal transduction pathways and/or transform the resultant gene expression patterns [32]. Since, the endogenous ROS levels are much higher in cancer cells therefore, an above threshold value to induce toxicity can be achieved faster than in normal cells [33, 34]. On the other hand, increased endogenous ROS are also responsible for tumorigenesis, metastasis, and resistance to radiation and chemotherapy [35, 36].

In this study, we examined the role of oxidative stress on A549 lung carcinoma cell line and their escape from immune responses. Here, the oxidative stress was achieved by implicating H_2O_2 treatment. However, H_2O_2 , a precursor to hydroxyl radical, is less reactive and more readily diffusible and thus more likely to be involved in the formation of oxidized bases [34]. From cytotoxicity assay, the 100 μM concentration of H_2O_2 was observed to be inducing oxidative stress without killing cells [37]. Differences in the protein profile on SDS-PAGE was observed in 24-h-oxidized cells when compared with the untreated control. These additional bands could be associated to the structural changes in protein subunits that might be possibly resulting into the formation of some neo-antigens. Other reports on neo-antigen density in non-small cell lung cancer and pulmonary premalignant conditions also support our claim that oxidative stress promoted neo-antigen formation [25, 38].

ROS and their secondary products disrupt the structure and conformation of biomolecules via different mechanisms. Addition of carbonyl derivatives to protein causes fragmentation of the polypeptide chain, which may lead to altered cellular functions such as energy production, interference with the membrane potentials, and partial to total loss of enzymatic activity [39]. Similarly, the peroxidation of polyunsaturated fatty acids of the cell membranes alters their permeability and fluidity and may also affect membrane-bound proteins [40–42]. Protein carbonyl and lipid peroxidation have emerged as potent biomarkers of oxidative stress and tissue damage resulting from chronic inflammation, in various physiological disorders including, cardiovascular diseases and cancer [43–45]. A higher protein carbonyl and TBARS (a by-product of lipid peroxidation) content in H_2O_2 -treated A549 cells in our study signified protein and membrane-lipid oxidation consistent to other reports

Fig. 4 Effect of Neo-antigen formation on phagocytosis. **a** Cells stained with Giemsa-exhibiting phagocytosis. The A549 cells treated with 100 μ M H_2O_2 for 15 min and for 24 h were co-cultured with THP-1 cells; In Control and 15 min H_2O_2 treatment, most of the A549 cells (elongated cells) are engulfed by THP-1 macrophages; whereas in 24 h H_2O_2 treatment, A549 cells escape from THP-1 macrophages. **b** The percent A549 cells engulfed by THP1 macrophages following H_2O_2 (100 μ M) treatments calculated as per the formula described in “Materials and methods.” **c** The CFSE pre-stained A549 cells treated with 100 μ M H_2O_2 for 15 min and for 24 h were co-cultured with THP-1 cells. Representative images of Phase contrast (A–C), CFSE stained (D–F), and merged pictures (G–I) exhibiting phagocytosis of A549 cells. **d** Figure showing the proportion of A549 cells engulfed by THP1 macrophages following H_2O_2 (100 μ M) treatments (significant at $*p < 0.05$)

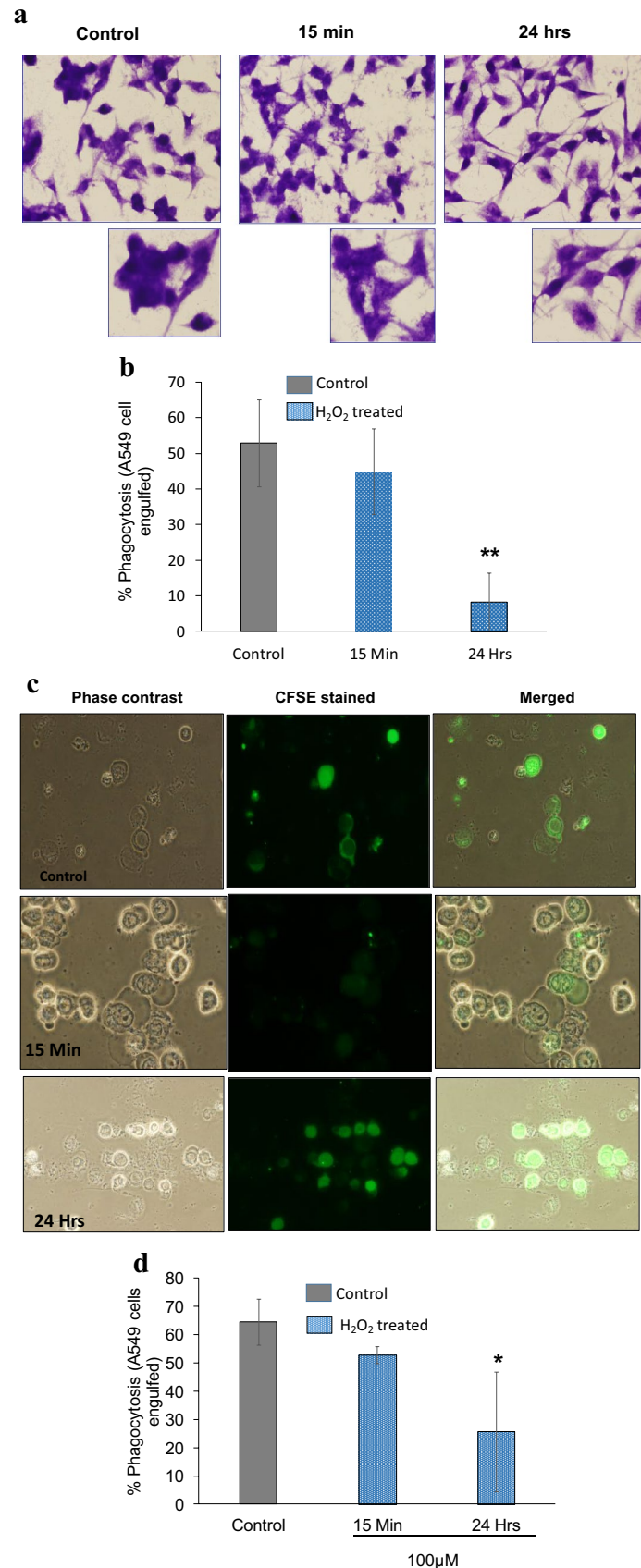
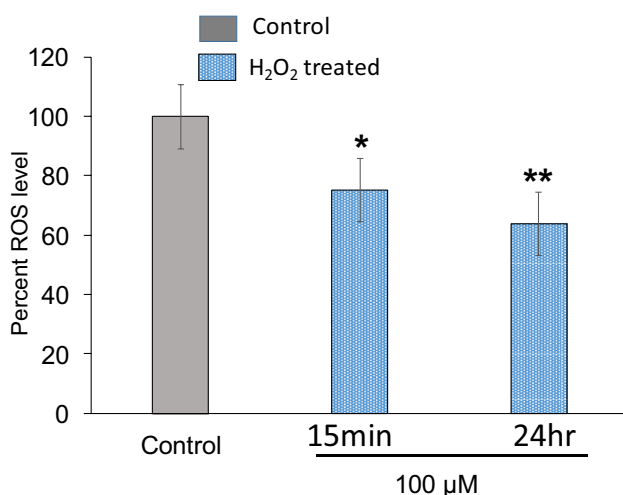


Table 2 The A549 cells treated with 100 μM H_2O_2 for 15 min and for 24 h were co-cultured with the THP-1 cells

Treatment	% Engulfed cells (Giemsa stain) Mean \pm SD	% Engulfed cells (CFSE-stained A549 cells) Mean \pm SD
Control	53 \pm 12.2	58 \pm 8.18
15 min H_2O_2 treatment	45 \pm 12.06	53 \pm 3.01
24 h H_2O_2 treatment	8 \pm 8.3**	25 \pm 14.52*

The number of engulfed A549 cells observed after the Giemsa and CFSE staining (significance at ** $p < 0.01$, * $p < 0.05$) are presented below

**Fig. 5** Effect of neo-antigen formation on respiratory burst. The A549 cells treated with 100 μM H_2O_2 for 15 min and for 24 h were co-cultured with THP-1 cells and the levels of ROS was detected using NBT assay. The results are expressed as the mean \pm standard deviation ($n = 3$). Student t test was performed to evaluate the significance of the results, the data were considered as statistically significant at * $p \leq 0.05$ and ** $p \leq 0.005$ when H_2O_2 -treated cells were compared with untreated controls**Table 3** The A549 cells treated with 100 μM H_2O_2 for 15 min and for 24 h were co-cultured with the THP-1 cells and NBT assay was performed to detect the ROS levels

Treatment	Percent ROS levels
Control	100 \pm 11
15 min H_2O_2 treatment	75 \pm 18*
24 h H_2O_2 treatment	63 \pm 10**

Table shows the percent ROS levels (arbitrary units) and the percent decrease in ROS levels (significant at * $p < 0.05$ and ** $p < 0.01$)

documenting the role of oxidative stress in promotion of tumorigenesis [46, 47]. Nitric oxide is produced enzymatically from L -arginine in the presence of NOS. The upregulation of inducible nitric oxide synthase (NOS2/iNOS) and

prolonged generation of NO during inflammatory responses are undoubtedly involved in tumorigenesis. Under the influence of a long duration oxidative stress, decrease in NOS2 expression was observed. It may be due to the fact that oxidative stress-induced lipid peroxidation results in the formation of 4HNE which further subtracts inducible nitric oxide synthase by inhibiting the NF- κ B activity. However, initially (15 min), the level of HNE might have been low which is reported by some previous groups [48, 49].

The human THP-1 (macrophage) cell line is a widely used in vitro model system for studying macrophages differentiation and function [50]. Macrophages participate in phagocytosis, respiratory burst, innate immune responses, initiate adaptive immunity, and also act as antigen presenting cell. However, ROS produced during phagocytosis can also change the morphological and marker expression and consequently contribute to tumor metastasis and invasion [51]. To demonstrate whether cancer cells can evade the macrophage attack after oxidation treatment in vitro, we employed Giemsa and CFSE staining. The 24 h-treated A549 cells co-cultured with THP1 cells showed interesting immune-escaping characteristics. Our experiments indicated that the induced amount of ROS favored the survival of A549 cells. From the protein profiles, it was further evident that ROS might have promoted the changes in antigen structure or conformation and hence, escaping from phagocytosis.

Phagocytes produce superoxide anion ($\text{O}_2^{\bullet-}$) and H_2O_2 via the intracellular enzymatic activity of NOX and superoxide dismutase during oxidative respiratory burst [52, 53]. These reactive molecules serve as inflammatory mediators constituting a part of host immune response activity by killing the invading pathogens [39]. Percent decrease in ROS levels detected by nitroblue tetrazolium (NBT) assay is an indirect measure of superoxide-dependent activity of the phagocytes [54]. Respiratory burst in THP-1 cells co-cultured with 24 h-treated A549 cells decreased significantly, whereas the 15 min treatment had minimal effect on ROS level. Furthermore, the THP-1 cells co-cultured with H_2O_2 -treated A549 cells for 24 h showed no change in p47^{phox} positive cells. From the normal flavocytochrome p47^{phox}, cytosolic component of NOX, it was inferred that the NOX function is unaffected during phagocytosis in the H_2O_2 -treated cells. It can be explained by considering the fact that other sources like, mitochondrial respiration, or xanthine oxidase system might cause the release of ROS inside the cancerous cells or macrophages [55, 56] and hence, activate the NOX. In past few years, different combination of approaches is in demand to understand the early diagnosis and better therapeutics for cancer. Present study is focused on the role of oxidative stress in formation of epitopes (neo-antigens) as well as their respective effect on innate immune responses. Although, additional prerequisite for the preclinical and clinical evidence are required

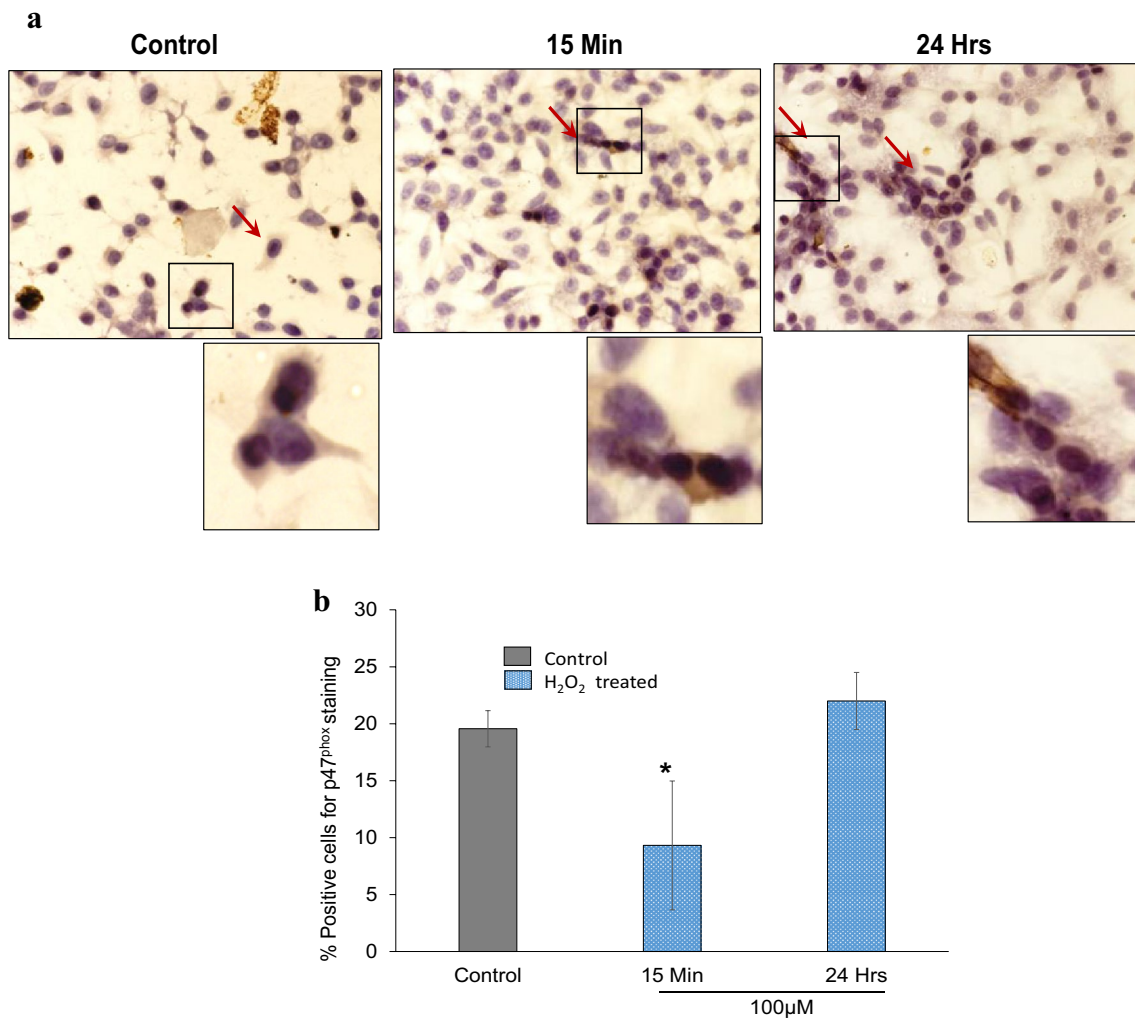


Fig. 6 Immunohistostaining for p47^{phox} (cytosolic unit of NADPH oxidase). The A549 cells treated with 100 μ M H₂O₂ for 15 min and for 24 h were co-cultured with THP-1 cells, and immunohistostaining for P47^{phox} was performed as described in “Materials and methods.”

a Representative images of the cells with positive staining (brown coloration) for P47^{phox}. **b** Percent cells with P47^{phox} positive staining. significant at * $p < 0.05$ and ** $p < 0.01$

Table 4 The A549 cells treated with 100 μ M H₂O₂ for 15 min and for 24 h were co-cultured with THP-1 cells and immunohistostaining for P47^{phox} was performed

Treatment	Percent positive cells Mean \pm SD	% Change in positive cells
Control	20 \pm 1.59	100
15 min H ₂ O ₂ treatment	9 \pm 5.66*	53*
24 h H ₂ O ₂ treatment	22 \pm 5.66	10

Table represents the percent positive for p47^{phox} staining and percent change for P47^{phox} staining (brown coloration) (significant at * $p < 0.05$ and ** $p < 0.01$)

but identifying these tumor-specific neo-antigens that are formed due to oxidative modifications and correlating them with clinical patient’s data will increase our understanding

of cancer pathogenesis, and will provide opportunities for the development of adjunct therapies to control progression of the disease and detect cancer at very initial stages.

Conclusion

Present work has characterized the pathological significance of neo-antigens and has established oxidative stress as a new pathogenic mechanism of carcinogenesis. This study will open new avenues for clinical intervention and adjunct therapies for cancer, and it also advocates for new ventures to increase the efficacy of the chemotherapeutic drugs through neo-antigen formation in the cancer cells. In future studies, we propose to identify these neo-antigens using proteomics-based studies and will validate their effect

on a number of more cancer cell lines to see their effect on immune responses.

Acknowledgements MD acknowledges the Fast Track Young Investigator Grant (SB/YLS/107/2013) from Dept. of Science and Technology, Govt. of India. The Junior Research fellowship (JRF) provided to SU from Indian Council for Medical Research (ICMR), New Delhi, India, is kindly acknowledged. The authors acknowledge Dr. Anil K. Mantha, Associate Professor, Centre for Animal Sciences, Central University of Punjab, Bathinda, for his critical and constructive comments and the editing of the MS. The Central Instrument Laboratory of Central University of Punjab is acknowledged for the confocal facility.

Compliance with ethical standards

Conflict of interest The authors declared that they have no conflict of interest.

References

- Gupta SC, Hevia D, Patchva S, Park B, Koh W, Aggarwal BB (2012) Upsides and downsides of reactive oxygen species for cancer: the roles of reactive oxygen species in tumorigenesis, prevention, and therapy. *Antioxid Redox Signal* 16:1295–1322
- Lotfy M, Sherif YE (2011) Free radicals and gastric cancer. Gastric carcinoma—molecular aspects and current advances. InTech, Rijeka:159–184
- England K, Cotter T (2005) Direct oxidative modifications of signalling proteins in mammalian cells and their effects on apoptosis. *Redox Rep* 10:237–245
- Fiaschi T, Chiarugi P (2012) Oxidative stress, tumor microenvironment, and metabolic reprogramming: a diabolic liaison. *Int J Cell Biol*. <https://doi.org/10.1155/2012/762825>
- Laurent A, Nicco C, Chereau C, Goulvestre C, Alexandre J, Alves A, Levy E, Goldwasser F, Panis Y, Soubrane O, Weill B, Batteux F (2005) Controlling tumor growth by modulating endogenous production of reactive oxygen species. *Cancer Res* 65:948–956
- Gurudath S, Naik RM, Ganapathy K, Guruprasad Y, Sujatha D, Pai A (2012) Superoxide dismutase and glutathione peroxidase in oral submucous fibrosis, oral leukoplakia, and oral cancer: a comparative study. *J Orofac Sci* 4:114–119
- Luanpitpong S, Talbott SJ, Rojanasakul Y, Nimmanit U, Pongrakhananon V, Wang L, Chanvorachote P (2010) Regulation of lung cancer cell migration and invasion by reactive oxygen species and caveolin-1. *J Biol Chem* 285:38832–38840
- Knaus UG (2002) The role of ROS in breast cancer metastasis. Defense Technical Information Centre Document
- Khandrika L, Kumar B, Koul S, Maroni P, Koul HK (2009) Oxidative stress in prostate cancer. *Cancer Lett* 282:125–136
- Herzer K, Sprinzl M, Galle PR (2007) Hepatitis viruses: live and let die. *Liver Int* 27:293–301
- Murray J, Oquendo CE, Willis JH, Marusich MF, Capaldi RA (2008) Monitoring oxidative and nitrate modification of cellular proteins; a paradigm for identifying key disease related markers of oxidative stress. *Adv Drug Deliv Rev* 60:1497–1503
- Chevon M, Berenshtein E, Stadtman E (2000) Human studies related to protein oxidation: protein carbonyl content as a marker of damage. *Free Radic Res* 33:S99–108
- Marquez A, Villa-Treviño S, Guéraud F (2007) The LEC rat: a useful model for studying liver carcinogenesis related to oxidative stress and inflammation. *Redox Rep* 12:35–39
- Upadhyay S, Sharma N, Gupta KB, Dhiman M (2018) Role of immune system in tumor progression and carcinogenesis. *J Cell Biochem* 119(7):5028–5042
- Goswami S, Sahai E, Wyckoff JB, Cammer M, Cox D, Pixley FJ, Stanley ER, Segall JE, Condeelis JS (2005) Macrophages promote the invasion of breast carcinoma cells via a colony-stimulating factor-1/epidermal growth factor paracrine loop. *Cancer Res* 65:5278–5283
- Meng D, Lv DD, Fang J (2008) Insulin-like growth factor-I induces reactive oxygen species production and cell migration through Nox4 and Rac1 in vascular smooth muscle cells. *Cardiovasc Res* 80:299–308
- Schmid MC, Varner JA (2010) Myeloid cells in the tumor microenvironment: modulation of tumor angiogenesis and tumor inflammation. *J Oncol*. <https://doi.org/10.1155/2010/201026>
- Zhang Y, Choksi S, Chen K, Pobeziinskaya Y, Linnoila I, Liu ZG (2013) ROS play a critical role in the differentiation of alternatively activated macrophages and the occurrence of tumor-associated macrophages. *Cell Res* 23:898–914
- Catera R, Silverman GJ, Hatzi K, Seiler T, Didier S, Zhang L, Hervé M, Meffre E, Oscier DG, Vlassara H (2008) Chronic lymphocytic leukemia cells recognize conserved epitopes associated with apoptosis and oxidation. *Mol Med* 14:665–674
- Sim Choi H, Woo Kim J, Cha YN, Kim C (2006) A quantitative nitroblue tetrazolium assay for determining intracellular superoxide anion production in phagocytic cells. *J Immunoassay Immunochem* 27:31–44
- Brown SD, Warren RL, Gibb EA, Martin SD, Spinelli JJ, Nelson BH, Holt RA (2014) Neo-antigens predicted by tumor genome meta-analysis correlate with increased patient survival. *Genome Res* 24:743–750
- Ramsey MR, Sharpless NE (2006) ROS as a tumour suppressor? *Nat Cell Biol* 8:1213–1215
- Anichini A, Tassi E, Grazia G, Mortarini R (2018) The non-small cell lung cancer immune landscape: emerging complexity, prognostic relevance and prospective significance in the context of immunotherapy. *Cancer Immunol Immunother*. <https://doi.org/10.1007/s00262-018-2147-7>
- Chae YK, Anker JF, Bais P, Namburi S, Giles FJ, Chuang JH (2018) Mutations in DNA repair genes are associated with increased neo-antigen load and activated T cell infiltration in lung adenocarcinoma. *Oncotarget* 9:7949–7960
- Anagnostou V, Smith KN, Forde PM, Niknafs N, Bhattacharya R, White J, Zhang T, Adleff V, Phallen J, Wali N (2017) Evolution of neoantigen landscape during immune checkpoint blockade in non-small cell lung cancer. *Cancer Discov* 7:264–276
- Neyen C, Plüddemann A, Mukhopadhyay S, Maniati E, Bossard M, Gordon S, Hagemann T (2013) Macrophage scavenger receptor promotes tumor progression in murine models of ovarian and pancreatic cancer. *J Immunol* 190:3798–3805
- Dhiman M, Zago MP, Nunez S, Amoroso A, Rementeria H, Dousset P, Burgos FN, Garg NJ (2012) Cardiac-oxidized antigens are targets of immune recognition by antibodies and potential molecular determinants in Chagas disease pathogenesis. *PLoS ONE* 7:e28449
- Gill I, Kaur S, Kaur N, Dhiman M, Mantha AK (2017) Phytochemical ginkgolide B attenuates amyloid- β 1-42 induced oxidative damage and altered cellular responses in human neuroblastoma SH-SY5Y cells. *J Alzheimers Dis* 60:S25–S40
- Dhiman M, Garg NJ (2011) NADPH oxidase inhibition ameliorates *Trypanosoma cruzi*-induced myocarditis during Chagas disease. *J Pathol* 225:583–596
- Ferlay J, Shin HR, Bray F, Forman D, Mathers C, Parkin DM (2010) Estimates of worldwide burden of cancer in 2008: GLOBOCAN 2008. *Int J Cancer* 127:2893–2917

31. Azad N, Rojanasakul Y, Vallyathan V (2008) Inflammation and lung cancer: roles of reactive oxygen/nitrogen species. *J Toxicol Environ Health Part B* 11:1–15
32. Klaunig JE, Kamendulis LM, Hocevar BA (2010) Oxidative stress and oxidative damage in carcinogenesis. *Toxicol Pathol* 38:96–109
33. Laurent A, Nicco C, Chéreau C, Goulvestre C, Alexandre J, Alves A, Lévy E, Goldwasser F, Panis Y, Soubrane O (2005) Controlling tumor growth by modulating endogenous production of reactive oxygen species. *Cancer Res* 65:948–956
34. Khan M, Ding C, Rasul A, Yi F, Li T, Gao H, Gao R, Zhong L, Zhang K, Fang X (2012) Isoalantolactone induces reactive oxygen species mediated apoptosis in pancreatic carcinoma PANC-1 cells. *Int J Biol Sci* 8:533–547
35. Shi X, Zhang Y, Zheng J, Pan J (2012) Reactive oxygen species in cancer stem cells. *Antioxid Redox Signal* 16:1215–1228
36. Ishikawa K, Takenaga K, Akimoto M, Koshikawa N, Yamaguchi A, Imanishi H, Nakada K, Honma Y, Hayashi J-I (2008) ROS-generating mitochondrial DNA mutations can regulate tumor cell metastasis. *Science* 320:661–664
37. Kim S-H, Kim K-H, Yoo B-C, Ku J-L (2012) Induction of LGR5 by H₂O₂ treatment is associated with cell proliferation via the JNK signaling pathway in colon cancer cells. *Int J Oncol* 41:1744–1750
38. Krysan K, Tran LM, Grimes BS, Walser TC, Wallace WD, Dubinett SM (2017) Evaluation of progression associated neoepitopes and immune contexture in pulmonary premalignancy. *Am Assoc Cancer Res* 77:1016
39. Silva JP, Coutinho OP (2010) Free radicals in the regulation of damage and cell death-basic mechanisms and prevention. *Drug Discov Ther* 4:144–167
40. Niki E, Yoshida Y, Saito Y, Noguchi N (2005) Lipid peroxidation: mechanisms, inhibition, and biological effects. *Biochem Biophys Res Commun* 338:668–676
41. Dalle-Donne I, Rossi R, Colombo R, Giustarini D, Milzani A (2006) Biomarkers of oxidative damage in human disease. *Clin Chem* 52:601–623
42. Rahman I, van Schadewijk AA, Crowther AJ, Hiemstra PS, Stolk J, MacNee W, De Boer WI (2002) 4-Hydroxy-2-nonenal, a specific lipid peroxidation product, is elevated in lungs of patients with chronic obstructive pulmonary disease. *Am J Respir Crit Care Med* 166:490–495
43. Kirkham PA, Spooner G, Ffoulkes-Jones C, Calvez R (2003) Cigarette smoke triggers macrophage adhesion and activation: role of lipid peroxidation products and scavenger receptor. *Free Radic Biol Med* 35:697–710
44. Dalle-Donne I, Rossi R, Giustarini D, Milzani A, Colombo R (2003) Protein carbonyl groups as biomarkers of oxidative stress. *Clin Chim Acta* 329:23–38
45. Popadiuk S, Renke J, Woźniak M, Korzon M (2005) Plasma protein peroxidation as a marker of oxidative stress intensity and antioxidant barrier activity in children who have completed treatment for neoplastic diseases. *Medycyna Wieku Rozwojowego* 10:849–854
46. Yeh C-C, Lai C-Y, Hsieh L-L, Tang R, Wu F-Y, Sung F-C (2010) Protein carbonyl levels, glutathione S-transferase polymorphisms and risk of colorectal cancer. *Carcinogenesis* 31:228–233
47. Bartling B, Hofmann H-S, Sohst A, Hatzky Y, Somoza V, Silber R-E, Simm A (2011) Prognostic potential and tumor growth-inhibiting effect of plasma advanced glycation end products in non-small cell lung carcinoma. *Mol Med* 17:980–989
48. Dijkstra G, Blokzijl H, Bok L, Homan M, van Goor H, Nico Faber K, Jansen PL, Moshage H (2004) Opposite effect of oxidative stress on inducible nitric oxide synthase and haem oxygenase-1 expression in intestinal inflammation: anti-inflammatory effect of carbon monoxide. *J Pathol* 204:296–303
49. Bowie AG, Moynagh PN, O'Neill LA (1997) Lipid peroxidation is involved in the activation of NF-κB by tumor necrosis factor but not interleukin-1 in the human endothelial cell line ecv304 lack of involvement of H₂O₂ in NF-κB activation by either cytokine in both primary and transformed endothelial cells. *J Biol Chem* 272:25941–25950
50. Grodzki ACG, Giulivi C, Lein PJ (2013) Oxygen tension modulates differentiation and primary macrophage functions in the human monocytic THP-1 cell line. *PLoS ONE* 8:e54926
51. Liu CY, Xu JY, Shi XY, Huang W, Ruan TY, Xie P, Ding JL (2013) M2-polarized tumor-associated macrophages promoted epithelial—mesenchymal transition in pancreatic cancer cells, partially through TLR4/IL-10 signaling pathway. *Lab Invest* 93:844–854
52. Sarna LK, Wu N, Hwang SY, Siow YL, O K (2010) Berberine inhibits NADPH oxidase mediated superoxide anion production in macrophages. This article is one of a selection of papers published in a special issue on Oxidative Stress in Health and Disease. *Can J Physiol Pharmacol* 88:369–378
53. Cathcart MK (2004) Regulation of superoxide anion production by NADPH oxidase in monocytes/macrophages contributions to atherosclerosis. *Arterioscler Thromb Vasc Biol* 24:23–28
54. James PE, Grinberg OY, Swartz HM (1998) Superoxide production by phagocytosing macrophages in relation to the intracellular distribution of oxygen. *J Leukoc Biol* 64:78–84
55. Kirkham P (2007) Oxidative stress and macrophage function: a failure to resolve the inflammatory response. *Biochem Soc Trans* 35:284–287
56. Bur H, Haapasaari KM, Turpeenniemi-Hujanen T, Kuitinen O, Auvinen P, Marin K, Koivunen P, Sormunen R, Soini Y, Karihtala P (2014) Oxidative stress markers and mitochondrial antioxidant enzyme expression are increased in aggressive Hodgkin lymphomas. *Histopathology* 65(3):319–327